communications in mathematical
match
and in computer chemistry

no. 38, October 1998

ISSN 0340-6253

MATCDY (38) 111-122 (1998)

Predatory Genetic Algorithms

F R Manby*, R L Johnston and C Roberts
School of Chemistry, University of Birmingham, Edgbaston
Birmingham B15 2TT, UK

June 22, 1998

Abstract

Genetic algorithms (GAs) have excelled in locating global minima, but in many instances other low-lying minima are sought. A method is introduced here which has the analogue of predation in natural evolution, and which is linked to a variational theory on a metric space. The method is used to find the two most stable structures of small Morse, Al_n and C_n clusters.

1 Introduction

The Genetic Algorithm (GA) is an optimization technique [1, 2] based on the principles of natural evolution [3]. The technique involves familiar evolutionary operations such as crossover, mutation and natural selection. In principle, the GA can be applied to any problem in which the quantity to be minimized (such as a potential energy, V) can be written as a function of a list of variables. Genetic nomenclature is employed in describing GAs, so the lists of variables are called chromosomes (each determining one individual), and each variable within a list corresponds to a gene.

GAs have been very successful in determining *global* minima, but in a number of physical applications, structures corresponding to higher local minima are very often of direct importance. For example, carbon cluster ions formed in laser-ablation experiments [4] are observed in several different geometries, distinguished by mobility. Also kinetically favoured, higher energy isomers may be formed, and the distribution of and interconversion between isomers is of great interest [5]. Finally, in aiming towards the optimization of protein structures, it is worth noting that the biologically active forms are often not at the global-minima [6, chapter 8].

*To whom correspondence should be addressed

Like the original idea of genetic algorithms [1], many of the subsequent developments have been inspired by natural evolution. For example, self-optimization [2, chapter 4] is clearly motivated by the way in which there are genes in nature which determine reproduction, for example by specifying mutation rates [7]. The relaxation of individuals into local minima corresponds to the pre-reproductive lifetime of the genetically determined individual (see for example [8]).

In this work the analogy is taken one step further by considering the use of predators to remove unwanted (although potentially minimal) individuals or traits from the population. Sometimes unwanted members of a population can be removed by imposing a constraint to the fitness function (figure 1a), however, in seeking minima other than the global minimum (figure 1b), where the derivatives of the *original* (unmodified) surface are required to vanish, a modification of the fitness function is not possible. An alternative solution is presented below.

Figure 1: Two different kinds of constraint. In (a) the constraint can be incorporated by modifying the fitness function f, but in (b), where a higher minimum in sought, there is no practical or general modification of the fitness function.

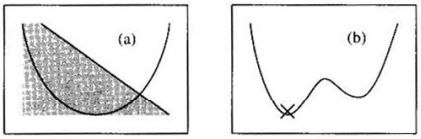

2 Theory I: The standard GA

Before considering the introduction of predators, the approach and notation for the GA will be summarized. Consider first the set of all possible *individuals* $\mathcal{I}$, of which the population at generation n is a subset

$$\mathcal{P}^{(n)} = \{p_i^{(n)} | i = 1, \ldots, n_{\text{pop}}\} \subset \mathcal{I}.$$

Let $\mathcal{P}$ be the set of all populations (the power set of $\mathcal{I}$), then $\mathcal{P}^{(n)} \in \mathcal{P}$. Consider also an operator ν for which $\nu\mathcal{P}^{(n)} = \mathcal{P}^{(n+1)}$. Each individual $p_i^{(n)} \in \mathcal{P}^{(n)}$ comprises an n_{gene}-tuple of objects from some set $\mathcal{D}$; as this work is applied to cluster geometries, $\mathcal{D}$ will be identified with $\mathbb{R}^3$, and n_{gene} with n_{atom}

The operator ν, which yields a new *generation*, is completely determined by:

1. The surface, $V\colon \mathcal{I} \to \mathbb{R}$
2. The fitness function, $f = \tilde{f}_{v_{\min}}^{v_{\max}} \circ V$, $f\colon \mathcal{I} \to (0, 1]$

3. A selection operator, σ: $\mathcal{P} \to \mathcal{S}$ where $\mathcal{S}$ is the power set of $\{(p, p') | p, p' \in \mathcal{I}, p \neq p'\}$
4. The mating operator, m: $\mathcal{S} \to \mathcal{P}$
5. The mutation operator, μ: $\mathcal{P} \to \mathcal{P}$
6. The relaxation operator, ρ: $\mathcal{P} \to \mathcal{P}$
7. The sorting operator, s: $\mathcal{P} \to \mathcal{P}$

V is typically a potential energy surface in a chemical application, and will in this work be identified with the Morse pair-potential [9] or the Murrell-Mottram potential [10]. The fitness function f is defined here in terms of

$$\tilde{f}_{v_{\min}}^{v_{\max}}(v) = \exp\left(\beta \frac{v_{\min} - v}{v_{\max} - v_{\min}}\right)$$

where $v = V(p)$ for some $p \in \mathcal{P}^{(n)}$,

$$\begin{aligned} v_{\min} &= \min_{p' \in \mathcal{P}^{(n)}} V(p') \qquad \text{and} \\ v_{\max} &= \max_{p' \in \mathcal{P}^{(n)}} V(p'). \end{aligned}$$

The parameter β determines the shape of the fitness function.

The selection operator randomly selects $n_{\text{pairs}} = \gamma n_{\text{pop}}$ pairs from the population with a probability determined by their fitness. Thus

$$\begin{aligned} \sigma\mathcal{P}^{(n)} = \Big\{ (p_i, p_j) \Big| & p_i = \text{rand}\mathcal{P}^{(n)}, p_j = \text{rand}\mathcal{P}^{(n)}, i \neq j, \\ & f(p_i) \leq \text{rand}(0,1], f(p_j) \leq \text{rand}(0,1], n_{\text{pairs}} = \gamma n_{\text{pop}} \Big\}. \end{aligned}$$

The parameter γ determines the proportion of the old population that will be allowed to survive: at least $\lfloor n_{\text{pop}}(1-\gamma) \rfloor$ individuals from $\mathcal{P}^{(n)}$ survive to form part of $\mathcal{P}^{(n+1)}$. In all calculations here $\gamma = 4/5$.

The mating operator m is based on single-point crossover at a random point (see figure 2), and operates on $\sigma\mathcal{P}^{(n)}$ to give

$$m\sigma\mathcal{P}^{(n)} = \{p_i^{(n)} \times p_j^{(n)} | (p_i^{(n)}, p_j^{(n)}) \in \sigma\mathcal{P}^{(n)}\}$$

where $p \times p'$ denotes the crossover of the two individuals. Specifically, writing $p = (p_1, p_2, \ldots, p_{n_{\text{gene}}})$ and a similar expression for p', the crossover is given by

$$p \times p' = (p_1, \ldots, p_k, p'_{k+1} \ldots, p'_{n_{\text{gene}}})$$

where $k = \text{rand}[1, n_{\text{gene}} - 1]$.

The mutation operator μ may randomly alter one individual in the population according to a probability parameter μ_{rate}. So

$$\mu\mathcal{P}^{(n)} = \begin{cases} \mathcal{P}^{(n)} & \text{if rand}(0,1] > \mu_{\text{rate}} \\ \{p_i^{(n)} \in \mathcal{P}^{(n)} | i \neq k\} \cup \{\tilde{\mu} p_k^{(n)}\} & \text{otherwise} \end{cases}$$

Figure 2: The crossover of two individuals p_1 and p_2 to a form a new individual $p' = p_1 \times p_2$.

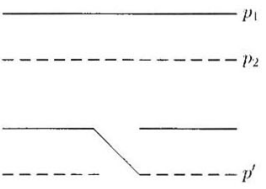

where $k = \text{rand}[1, \gamma n_{\text{pop}}]$. The effect of $\tilde{\mu}$ on an individual is to replace $\lfloor n_{\text{gene}}/3 \rfloor$ (randomly chosen) elements of the n_{gene}-tuple with random values from $\mathcal{D}$.

The relaxation operator ρ performs a quasi-Newton minimization of the individuals on the surface V, and the individuals are then sorted (s) in order of decreasing fitness. The overall operator ν for the standard GA is given by

$$\nu = s \cdot \rho \cdot \mu \cdot m \cdot \sigma.$$

3 Theory II: The predatory GA

The standard GA, defined above in terms of an operator ν, is modified to incorporate a predation operator $\pi : \mathcal{P} \to \mathcal{P}$ to yield the predatory GA (PGA), $\nu_\pi = \pi \cdot \nu$. The predator removes individuals from a population based on proximity to a fixed individual. This necessitates some metric on $\mathcal{I}$, $d : \mathcal{I}^2 \to [0, \infty)$, forming the metric space $(\mathcal{I}, d)$. Then the predation operator π removes individuals from the population if they are closer than some threshold ϵ_π to the fixed individual p_0. The action of π on $\mathcal{P}^{(n)}$ is then

$$\pi\mathcal{P}^{(n)} = \{p \in \mathcal{P}^{(n)} | d(p, p_0) \geq \epsilon_\pi\}$$

The strategy is to find p_0, the individual at the global minimum, using the standard GA, then to use the PGA to compute the second lowest minimum.

The PGA is related to a variational theory for higher eigenvalues. The lth eigenvalue of an operator can be computed by imposing orthogonality constraints between the lth eigenfunction and the $l-1$ lower eigenfunctions [11, 12]; in this work a higher energy minimum is computed by ensuring a large distance from p_0. As in the eigenvalue problem, one need not stop at the second lowest minimum, the lth lowest one being given by

$$\pi_l\mathcal{P}^{(n)} = \{p \in \mathcal{P}^{(n)} | d(p, p_0) \geq \epsilon_\pi, \ldots, d(p, p_{l-1}) \geq \epsilon_\pi\}$$

with p_i arising from the PGA requiring only π_{i-1}. In this way finding successive minima of V by building π_0 (ie the identity), π_1 (ie the predator operator applied in this work),

π_2, etc, amounts to a variation theorem on a metric space. The orthogonality constraint, imposed in a variational theorem on Hilbert space by a vanishing inner product, is replaced by a distance constraint on a metric space. Indeed, if the minimization is taken to require that the derivatives of V with respect to all variable directions vanish, then the threshold ϵ_π is arbitrary, except that $\epsilon_\pi > 0$.

In the present calculations the GA and PGA are applied to cluster geometry optimization, where each individual consists of n_{atom} genes, each being a 3-vector specifying the location of an atom: $\mathcal{D} = \mathbb{R}^3$. The GA is based on the work of Deaven *et al.* [8], wherein the mating (crossover) procedure is accomplished by 'slicing' a pair of clusters and joining together the complementary fragments. Here, the clusters are subjected to a random reorientation, and the slicing is performed with respect to atom positions along the z-axis. To prevent the generation of clusters having pairs of atoms very close together, a partial local minimization is carried out on each child cluster (by the relaxation operator, ρ). The method, including a number of modifications that we have introduced, will be described more fully in a forthcoming publication [13].

Two forms for the surface, or potential energy function, V are considered in this work: the two-body Morse potential [9], and the [2 + 3]-body Murrell-Mottram potential [10]. The Morse potential is defined with $D_e = -1$ and $r_e = 1$ to give

$$V_{ij} = e^{\alpha(1-r_{ij})}[e^{\alpha(1-r_{ij})} - 2]$$

and the scaling parameter α is set to 6. The coefficients of the Murrell-Mottram potential [10] are taken from Eggen *et al.* [14] for carbon clusters, and from Lloyd and Johnston [15, table 1] for the aluminium clusters. The exact form of the MM potential and values of the parameters for a number of elements can be found in a recent review [16].

The metric function d then needs to be constructed for the special case of cluster geometries, and this presents a problem: the clusters produced in the (P)GA have a random orientation, and reorientation to minimize the deviation of atomic positions would be an extremely time consuming step. However, consider the interparticle distance matrix $\mathbf{D}$ for a single cluster, having elements $D_{ij} = [(x_i - x_j)^2 + (y_i - y_j)^2 + (z_i - z_j)^2]^{1/2}$. Note that $\mathbf{D}$ is invariant under all rotations of the cluster. But a problem still remains: the atoms are arbitrarily labelled. In other words, direct comparison of $\mathbf{D}$-matrices for clusters is only realistic to within an unknown permutation, P. Thus one should consider $\mathbf{P}^T\mathbf{D}\mathbf{P}$ where $\mathbf{P}$ is the matrix representing P. But permutation matrices are real and unitary and so $\mathbf{P}^T\mathbf{D}\mathbf{P} = \mathbf{P}^{-1}\mathbf{D}\mathbf{P}$, and it is immediately clear that $\mathbf{P}^T\mathbf{D}\mathbf{P}$ is similar to $\mathbf{D}$. Consequently, the eigenvalues of $\mathbf{D}$ are invariant not only under rotations but also under permutations of the labelling scheme.

It is then an easy step to construct an appropriate metric d. Writing $\mathbf{D}(p)$ for the interparticle distance matrix for the individual p, and denoting by spec $\mathbf{D}$ the (ordered) list of eigenvalues of $\mathbf{D}$, the metric is defined

$$d(p_i, p_j) = N\left[\sum_{k=1}^{n_{\text{atoms}}} \left([\text{spec}\,\mathbf{D}(p_i)]_k - [\text{spec}\,\mathbf{D}(p_j)]_k\right)^2\right]^{1/2}$$

where N is some suitable normalization constant. The efficacy of this metric will be demonstrated below in numerous examples.

4 Results

The results are presented in terms of potential energy and *average binding energy*, that is the binding energy per atom, defined as $E_b = -V(p)/n_{\text{atom}}$.

The GA and PGA has been applied to Morse clusters with $n_{\text{atom}} = 8, 9, 10$ and with $\alpha = 6$. The two most stable isomers (those with the highest E_b values) are listed in table 1 and their structures are shown in figure 3. The structures and energies of the global minima are identical with those reported by Doye *et al.* in an earlier study [17], but note the error in table I of [17], in which the energy for the 9B cluster ($\rho_0 = 6$) is given incorrectly. (The correct value is shown in table 1). For $n_{\text{atom}} = 9$ both isomers are bicapped pentagonal bipyramids, with a marked preference for the 1,2-isomer in which the two capping atoms are bonded to each other.

The two most stable isomers for the aluminium clusters with $n_{\text{atom}} = 5$ 10 are listed in table 2 and their structures are shown in figure 4. The structures and energies of the global minima are identical to those obtained previously, using a combination of random searching and Monte Carlo Simulated Annealing, by Lloyd and Johnston [15]. It is interesting to note that the PGA has enabled the identification of the pseudo-spherical bicapped square antiprism as the lowest metastable isomer of Al_{10}. This geometry is the ground state structure of the $[B_{10}H_{10}]^{2-}$ anion and is also found to be the global minimum for clusters bound with long-ranged (ie small-α) Morse potentials [17].

The two most stable isomers for several carbon clusters with 5 to 20 atoms are listed in table 3 and their structures are shown in figure 5. The lowest energy isomers are, in all cases, at least as stable as those found previously by Eggen *et al.* [14] and by another GA study (using the same potential) [18]. In the case of C_{18} our global minimum has a higher binding energy than that reported in [18]. The PGA also shows that, for C_5 and C_8 C_{18}, fragments of the pentagonal dodecahedron (the smallest fullerene and the global minimum for C_{20}) correspond either to the most stable or second most stable isomers — with the exception of C_{16}. It has been confirmed that the dodecahedral fragment isomer of C_{16} lies at a higher energy than those reported in table 3 and figure 5. Further studies are currently underway to explore the potential energy surface of carbon clusters (especially fullerenes) using the Murrell-Mottram potential and the PGA [13].

5 Conclusions

A GA-based method has been introduced for computing minima other than the global minimum, and has been shown to be a valuable method for computing low-lying structural

Table 1: Potential energies, binding energies and geometries of the lowest and second lowest M_n Morse clusters for $n = 8, 9$ and 10 and with $\alpha = 6$. Note that the energy values are dimensionless as $D_e = -1$. The notation $1,2$ and $1,1'$ denotes capping on adjacent sites above the plane, and opposite sites above and below the plane respectively. The diagrams in figure 3 clarify the meaning.

n	Energy	E_b		Geometry
8	−19.32742	2.4159	C_s	capped pentagonal bipyramid
	−19.16186	2.3952	D_{2d}	dodecahedron
9	−23.41719	2.6019	C_{2v}	1,2-bicapped pentagonal bipyramid
	−22.48804	2.4986	C_{2v}	1,1′-bicapped pentagonal bipyramid
10	−27.47328	2.7473	C_{3v}	tricapped pentagonal bipyramid
	−26.58405	2.6584	D_{2d}	hexadecahedron

Figure 3: Geometries of the lowest energy (left) and second lowest energy (right) clusters using the Morse potential with $\alpha = 6$.

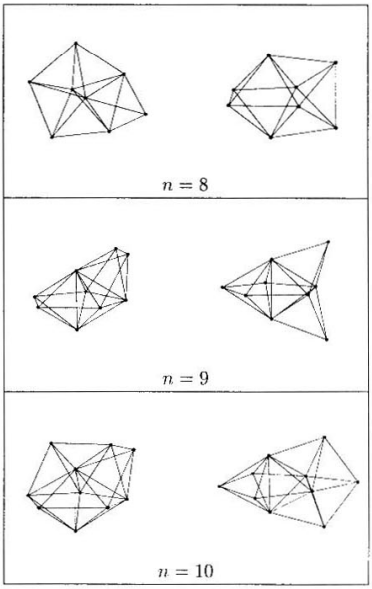

Table 2: Potential energies, binding energies and geometries of the two most stable Al_n clusters for $n = 5$–10.

n	Energy/eV	Stability/eV		Geometry
5	−6.62332	1.3247	D_{3h}	trigonal bipyramid
6	−9.02323	1.5038	O_h	octahedron
	−8.70553	1.4509	C_{2v}	bicapped tetrahedron
7	−11.23139	1.6044	D_{5h}	pentagonal bipyramid
	−11.09304	1.5847	C_{3v}	capped octahedron
8	−13.53835	1.6922	D_{2d}	dodecahedron
	−13.31247	1.6640	C_s	capped pentagonal bipyramid
9	−15.87643	1.7640	D_{3h}	tricapped trigonal prism
	−15.82299	1.7581	C_{2v}	bicapped pentagonal bipyramid
10	−18.28230	1.8282	C_{3v}	tricapped pentagonal bipyramid
	−18.19711	1.8197	D_{4d}	bicapped square antiprism

Table 3: Potential energies, binding energies and geometries of the two most stable isomers of selected C_n clusters.

n	Energy/eV	Stability/eV	Geometry
5	−27.80570	5.5611	pentagon
	−23.42532	4.6850	distorted kite
6	−33.72028	5.6200	chair hexagon
	−33.71246	5.6187	boat hexagon
7	−39.78155	5.6830	bicyclo[2.2.1]
	−39.41532	5.6307	chair heptagon
8	−47.78822	5.9735	bicyclo[3.3.0]
	−47.75892	5.9698	bicyclo[2.2.2]
9	−53.96306	5.9958	bicyclo[3.2.2]
	−53.93408	5.9926	bicyclo[3.3.1]
10	−62.12397	6.2123	T_d adamantane
	−62.00199	6.2001	dodecahedral fragment
12	−76.35192	6.3626	C_{2v}
	−76.20957	6.3507	dodecahedral fragment
14	−90.89410	6.4924	C_{2v}
	−90.37457	6.4553	dodecahedral fragment
15	−99.03808	6.6025	D_{5h}
	−98.87779	6.5918	dodecahedral fragment
16	−105.9045	6.6190	C_s
	−105.7367	6.6085	C_1
18	−121.5245	6.7513	C_2
	−121.4569	6.7476	dodecahedral fragment
20	−140.5065	7.0253	dodecahedron
	−136.9234	6.8461	C_1

Figure 4: Geometries of the lowest energy (top) and second lowest energy (bottom) Al_n clusters, using the potential described in the text. Note that there is only one minimum for Al_5.

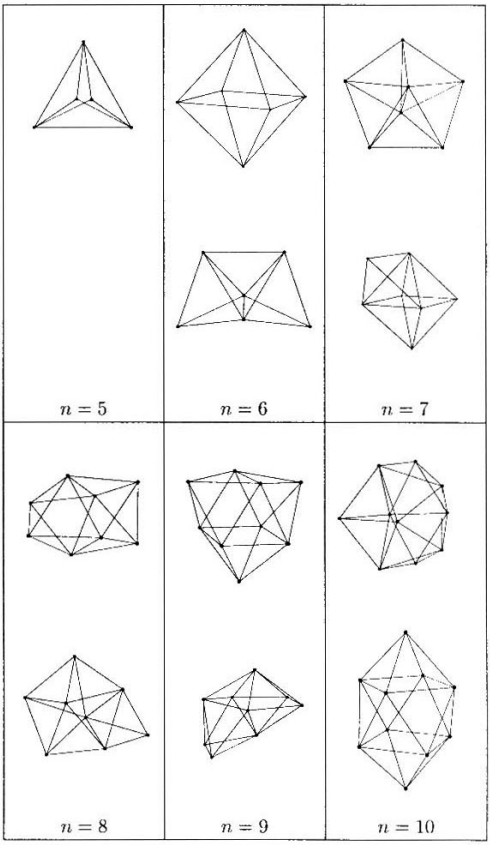

Figure 5: Geometries of selected C_n clusters. The lowest energy clusters are shown on the left, and the second lowest on the right.

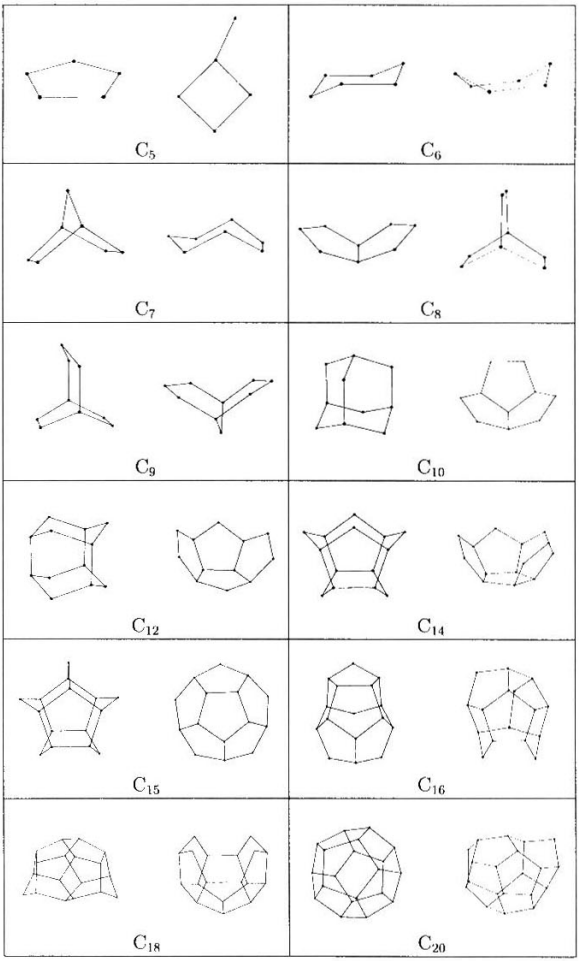

isomers of clusters. In addition to this application, the predator can considerably enhance the convergence of a GA if a structure is suspected *not* to be the global minimum, despite being the result of a GA optimization, a predator to remove it will often result in convergence to the true global minimum. In other words, the predator can be used to prevent premature convergence into deep, but non-global minima.

An alternative application would be to the problem of shape selectivity: it is possible to use a predator to remove individuals from the population if they show (or fail to show) certain topological pre-requisites such as sphericity, ring size and adjacent/non-adjacent pentagons. Future work will include the use of such shape-selective predators to compute the structure of isomers with specific features.

6 Acknowledgments

FRM and CR would like to thank the EPSRC for financial support.

References

[1] J Holland, *Adaptation in Natural and Artificial Systems* (Michigan, Ann Arbor, 1975)

[2] D E Goldberg, *Genetic Algorithms in Search, Optimization, and Machine Learning* (Addison-Wesley, Reading MA, 1989)

[3] C Darwin, *The Origin of Species* ed J B Burrow (Penguin, Baltimore, 1968) (reprinted from the first edition, 1859)

[4] G von Helden, M-T Hsu, P R Kemper and M T Bowers, *J. Chem. Phys.* **95** 3835 (1991)

[5] J P K Doye and D J Wales, *Phys. Rev. Letts.* **80** 1357 (1998)

[6] A R Leach, *Molecular Modelling: Principles and Applications* (Addison Wesley Longman, Harlow, 1996)

[7] A Aafif and J Lin, *Phys. Rev. E* **57** 2471 (1998)

[8] D M Deaven, N Tit, J R Morris and K M Ho *Chem. Phys. Letts.* **256** 195 (1996)

[9] P M Morse, *Phys. Rev.* **34** 57 (1929)

[10] J N Murrell and R E Mottram, *Mol. Phys.* **69** 571 (1990)

[11] C Eckart, *Phys. Rev.* **36** 878 (1930)

[12] A Weinstein and W Stenger, *Methods of Intermediate Problems for Eigenvalues*, (Academic Press, New York, 1972)

[13] C Roberts, R L Johnston and F R Manby, manuscript in preparation

[14] B R Eggen, R L Johnston and J N Murrell, *J. Chem. Soc. Farad. Trans.* **90** 3029 (1994)

[15] L D Lloyd and R L Johnston, *Chem. Phys.* in press (1998)

[16] H Cox, R L Johnston and J N Murrell, manuscript in preparation

[17] J P K Doye, D J Wales and R S Berry, *J. Chem. Phys* **103** 4234 (1995)

[18] S Hobday and R Smith, *J. Chem. Soc. Farad. Trans.* **93** 3919 (1997)